PHYS2041 Lab Report 2
Photoelectric Effect Due to Mercury Visible Spectra

Ryan White
s4499039

8th of October, 2021

Abstract

Using a two-stage experimental setup, the photoelectric effect for 3 visible wavelengths of light (from a mercury lamp) was investigated. After finding the stopping voltage for each of the 3 incident wavelengths of light (436nm, 546nm, and 577nm), a linear regression was performed that resulted in the work function of the experimental anode being found, as well as an estimate for Planck's constant that was reasonably consistent with currently agreed upon values; $\phi = 1.58 \pm 0.94$V and $h = 7.02 \pm 0.26 \times 10^{-34}$ J.s respectively. . Next, the current-voltage characteristic curve was plotted which showed a clear relationship between induced current and incident light frequency. From this, numerical methods were used to approximate the derivative of this curve, and thus the photoelectron kinetic energy distribution. Inferences were made as to the shape of the distribution, with limitations to the results described throughout the text.

1 Introduction

The photoelectric effect describes the process by which *photoelectrons* are created: electrons broken away from atoms of some material via the absorption of photons. Discovered in 1887 by Heinrich Hertz [2], the photoelectric effect was an essential building block in the advent of quantum mechanics and the quantization of light by the discovery of photons. With the subsequent scientific discourse of the effect, the idea of the wave-particle duality of light was validated and technological advances made possible [such as with image sensors, photoelectron spectroscopy and identification of charge of objects in a vacuum]. This experiment aimed to understand how different frequencies of light affect the induced current created by the photoelectric effect, and the consequent energy distribution of the photoelectrons created. Simultaneously, analysis of the stopping voltage with respect to frequency was used to determine Planck's constant with associated uncertainty.

2 Theory

As briefly described in the introduction, the photoelectric effect describes the process by which valence electrons of some material absorb sufficiently energetic photons, consequently detaching from their atom (influencing the charge of said atom) and inducing a current in a circuit. The process is a direct result of the quantum model of light in which light travels in discrete packets of energy, 'quanta', and is either absorbed or rejected completely by an atom (leading to a higher energy valence electron, or nothing respectively). The voltage at which photoelectrons begin to eject from a material under the influence of incident light is directly proportional to the *spatial* frequency (more precisely the angular wave number, k) of the incident light (which is directly proportional to the energy of the light). Dividing both sides of equation (2) from the laboratory notes by e gives this relationship:

$$V_{\text{cut-off}} = \frac{hc}{2\pi e} k - \phi \tag{1}$$

and define the quantity

$$m_{Vk} = \frac{hc}{2\pi e} \tag{2}$$

as the gradient of the voltage-frequency curve. Using this relationship, the value of Planck's constant can be found by rearranging and using known constants:

$$h = \frac{2\pi e}{c} m_{Vk} \tag{3}$$

Looking again at equation 1, the quantity ϕ refers to the work-function of the material releasing photoelectrons − the minimum work needed to remove an electron from the surface of the material [2]. Clearly equation 1 is of the form of a straight line (with the aforementioned gradient) with intercept ϕ, and so identifying this intercept allows for inferences of the photoelectron source material.

Over some range of voltage greater than the cut-off voltage, $V_{\text{cut-off}}$, a characteristic current-voltage curve, $i(V, \nu)$, is present - the shape of which is dependent upon the frequency of the incident light and the material from which the photoelectrons originate. The incident light frequency directly correlates with the kinetic energy of the ejected photoelectrons, with a higher light frequency corresponding to a higher photoelectron kinetic energy. It follows that the photoelectron kinetic energy distribution directly influences the induced current, as the current is the net flow rate of electrons and a higher kinetic energy translates to a higher rate of flow. The photoelectron kinetic energy distribution can be found by the derivative of the current-voltage curve in theory. In practice, numerical methods must be used to determine this derivative from the *observed* current-voltage curve and Sauer (2018) provided a good resource for numerical methods. The two-point differentiation formula [1] was derived from the 'rise over run' method of finding the average rate of change for some step size h:

$$\frac{dy}{dx} \simeq \frac{y_2 - y_1}{x_2 - x_1} \Rightarrow f'(x) \simeq \frac{f(x+h) - f(x)}{h} \tag{4}$$

where the denominator in the above reduces to h since $x_2 = x + h$ and $x_1 = x$. Sauer details that the optimal step-size in MATLAB is approx $h = 10^{-5}$, which corresponds to the sweet-spot between minimising calculation (floating point) error and maximising the number of points observed (in order to *approximate* a smooth curve). In practice, this level of accuracy wasn't feasible, with the finest detail being of the order of $h \propto 10^{-3}$.

3 Experiments

The experimental setup for the first phase of the experiment was shown in Figure 1.

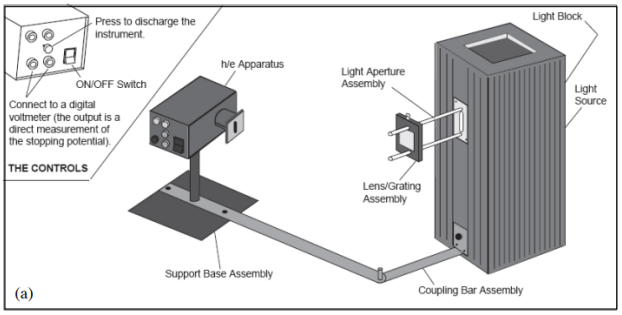

(a) Equipment Setup

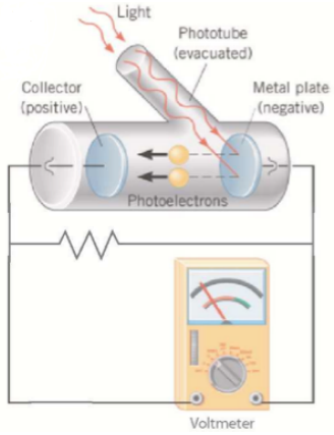

(b) Experiment Circuit Configuration

Figure 1: Stopping Voltage Experiment Setup

Figure 1b shows the physical processes involved in the apparatus. Energetic photons strike an anode (negatively charged metal plate), which induces a current of photoelectrons flowing towards a cathode (positively charged metal plate). This induced current has an inherent voltage which is measured with a voltmeter in parallel to a resistor.

Figure 2: Current-Voltage Curve Experiment Setup

Figure 2 shows the experimental setup of the second phase of the experiment. Used were 2 wavelength filters of 436nm and 577nm, a spectral mercury lamp, a photodiode detector, a digital voltmeter, and a sensitive picoammter.

3.1 Method

For the first experiment the mercury lamp was switched on and left to heat up for 10 minutes. All of the respective cables were plugged into the voltmeter, and the opening slit blocked so that the voltmeter could be calibrated to read 0V with no incident light. As per Appendix A, each of the spectral lines from the lamp were identified according to their angular position and intensity. The most prominent mercury spectral lines were observed (436, 546, and 577nm) and the support base assembly was rotated about the pivot such that the 436nm (blue) spectral line was entering through the slit on the h/e apparatus. The 100% intensity filter was placed over the slit, and the stopping voltage was recorded from the readout. This was repeated for the 80, 60, 40, and 20% intensity filters respectively. The 100% intensity filter was then placed over the slit once more to record a second trial, and the whole process repeated. This was repeated 4 times for a total of 5 trials of the stopping voltages with respect to intensity of 436nm light.
The filter was then removed from the slit, and the unimpeded stopping voltage recorded for 436nm light. Once recorded, the support base assembly was then rotated about the pivot such that the 546nm light was incident on the slit opening, and stopping voltage recorded. This was repeated for the 577nm spectral line, finishing by rotating the support base assembly back to the 436nm angular position. The process was

repeated 4 times for a total of 5 independent trials − the data of which was shown in Table 1.

The second part of the experiment involved varying voltage and observing the induced current produced by photoelectrons. Firstly, the lamp was turned on and left to warm up for 10 minutes. In this time, the appropriate cables on the ammeter and voltmeter were connected. The equipment was calibrated by adjusting the current calibration dial until the current reading was 0. Once the lamp had warmed up, the 436nm filter was placed over the entrance slit, and the voltage reduced to -2.5V. The current reading was taken for each 0.1V increment (starting at -2.5V, increasing linearly for the blue light). This was repeated up to a final voltage of 2.5V. The blue light filter was then removed, and the 577nm (yellow) filter placed on the entrance slit. The voltage was reduced down to -2.5V, and the associated current recorded. Over the range -2.2V $\rightarrow -1.0$V, the current was recorded in 0.2V increments. From -1.0V $\rightarrow -0.50$V, the current was recorded in 0.05V increments. Then, in the range -0.50V $\rightarrow$ 2.5V, the current was recorded in 0.1V increments, finally being recorded in 2.5V increments over the range 2.5V $\rightarrow$ 30V. The data taken was shown in Table 2.

3.2 Uncertainties

As with any experiment, this investigation of the photoelectric effect carried with it some inherent uncertainties in the data recorded. These uncertainties were reasonably low considering the nature of how data points were determined: electronic readouts using precise equipment. For the first phase of the experiment, the only data taken was of the form of a voltage from a voltmeter correct to one thousandth of a volt. This would imply an uncertainty of ± 0.001V, but was increased to ± 0.002V to account for minor fluctuations in the readout. The uncertainty in the mean of these values was calculated according to the formulae in Appendix B. Since the spectral lines of mercury are well known and were well defined (due to large angular separation caused by lens through which they were dispersed), there was no uncertainty in the spectral line being observed through the slit.

The second phase of the experiment carried with it comparatively more uncertainty in the data due to two independent variables being measured as opposed to one. The voltage being measured did carry with it some uncertainty (specifically ± 0.05V from the significant figures of the readout), but was ignored due to the predictable and precise way in which the voltage was changed. The current reading, however, was much more imprecise and was observed to regularly fluctuate between values. In this case, the uncertainty was taken to be the larger of either the smallest significant figure, or the range of fluctuation from some mean of the fluctuation.

In both phases of the experiment, the intensity and colour filters were supplied with no quoted uncertainty ranges and the uncertainties of them were consequently deemed negligible. Although colour filters were used for the bulk of the data collection, the experiments were performed in dark-room conditions to further prevent the contamination of data by background light.

4 Results

The tabulated data from the first phase of the experiment is shown in Table 1:

Colour	Intensity (%)	Voltage (V) ±0.002V					
		Trial 1	Trial 2	Trial 3	Trial 4	Trial 5	Mean
Blue (436nm)	100	-1.405	-1.403	-1.405	-1.406	-1.406	-1.405 ± 0.0005
	80	-1.398	-1.396	-1.401	-1.401	-1.399	-1.399 ± 0.0005
	60	-1.386	-1.384	-1.391	-1.392	-1.389	-1.388 ± 0.0005
	40	-1.374	- 1.366	-1.378	-1.379	-1.386	-1.377 ± 0.0005
	20	-1.315	-1.289	-1.320	-1.310	-1.322	-1.311 ± 0.0005
Blue (436nm)	N/A	-1.431	-1.438	-1.427	-1.428	-1.436	-1.432 ± 0.0005
Green (546nm)	N/A	-0.808	-0.808	-0.808	-0.807	-0.807	-0.808 ± 0.0005
Yellow (577nm)	N/A	-0.711	-0.707	-0.710	-0.702	-0.703	-0.707 ± 0.0005

Table 1: Stopping Voltage Results

Performing a linear regression on the last 3 rows of Table 1 yields

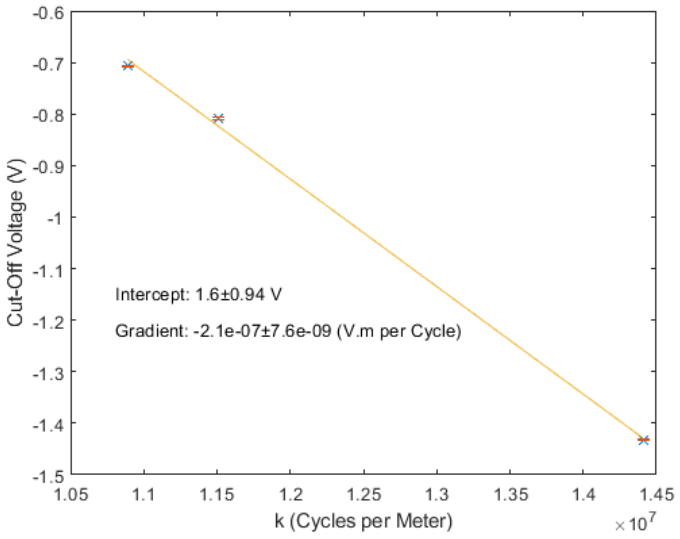

Figure 3: Stopping Voltage vs Spatial Frequency of Incident Photons

The tabulated data for the second phase of the experiment was shown in Table 2:

Voltage (V)	Filter	
	436nm Current ($\times 10^{-11}$A)	577nm Current ($\times 10^{-11}$A)
-2.5	-18 ± 1	-11.8 ± 0.2
-2.4	-18 ± 1	
-2.3	-18 ± 1	
-2.2	-18 ± 1	-11.8 ± 0.2
-2.1	-18 ± 1	
-2.0	-18 ± 1	-11.6 ± 0.2
-1.9	-18 ± 1	
-1.8	-18 ± 1	-11.7 ± 0.2
-1.7	-17 ± 1	
-1.6	-16 ± 1	-11.6 ± 0.2
-1.5	-14 ± 1	
-1.4	-10 ± 1	-11.7 ± 0.2
-1.3	-2 ± 1	
-1.2	7 ± 1	-11.8 ± 0.2
-1.1	27 ± 1	
-1.0	61 ± 1	-11.4 ± 0.2
-0.95		-10.2 ± 0.1
-0.90	86 ± 1	-9.9 ± 0.1
-0.85		-9.8 ± 0.1
-0.80	128 ± 2	-9.7 ± 0.1
-0.75		-9.0 ± 0.1
-0.70	178 ± 1	-7.5 ± 0.1
-0.65		-3.5 ± 0.1
-0.60	236 ± 2	4.4 ± 0.1
-0.55		16.7 ± 0.2
-0.50	280 ± 2	32.2 ± 0.4
-0.4	298 ± 3	74 ± 1
-0.3	363 ± 5	127 ± 1
-0.2	405 ± 5	159 ± 1
-0.1	445 ± 6	185 ± 1
0.0	498 ± 6	253 ± 1
0.1	598 ± 8	316 ± 3
0.2	635 ± 8	341 ± 5

Voltage (V)	Filter	
	436nm Current ($\times 10^{-11}$A)	577nm Current ($\times 10^{-11}$A)
0.3	715 ± 15	385 ± 3
0.4	745 ± 13	434 ± 5
0.5	810 ± 10	470 ± 8
0.6	873 ± 7	510 ± 10
0.7	900 ± 6	550 ± 10
0.8	980 ± 20	590 ± 10
0.9	1000 ± 20	630 ± 10
1.0	1050 ± 10	660 ± 10
1.1	1080 ± 30	710 ± 10
1.2	1160 ± 20	740 ± 10
1.3	1220 ± 20	770 ± 10
1.4	1260 ± 20	800 ± 10
1.5	1340 ± 20	840 ± 10
1.6	1390 ± 20	880 ± 10
1.7	1440 ± 20	910 ± 10
1.8	1510 ± 30	930 ± 10
1.9	1520 ± 20	970 ± 10
2.0	1580 ± 20	990 ± 10
2.1	1660 ± 30	1010 ± 10
2.2	1730 ± 20	1060 ± 10
2.3	1790 ± 20	1070 ± 10
2.4	1860 ± 30	1110 ± 10
2.5	1940 ± 20	1130 ± 10
5.0		2000 ± 40
7.5		2440 ± 50
10.0		3000 ± 100
12.5		3300 ± 100
15.0		3600 ± 100
17.5		3800 ± 100
20.0		4000 ± 100
22.5		4100 ± 100
25.0		4300 ± 100
27.5		4400 ± 100
30.0		4500 ± 100

Table 2: Induced Current vs Voltage for Photoelectrons

Plotting this data gives the characteristic current-voltage curve induced by the photoelectrons:

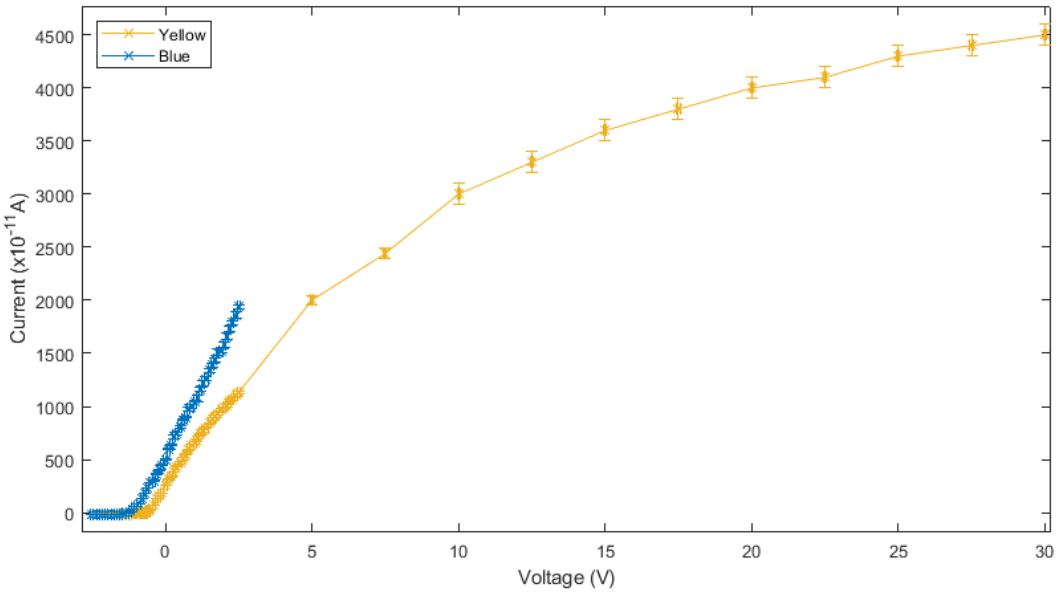

Figure 4: Current-Voltage Characteristic Curve

Calculating the instantaneous derivative at each of the data points in Figure 4 by the numerical method explained in the theory section gives the photoelectron energy distribution:

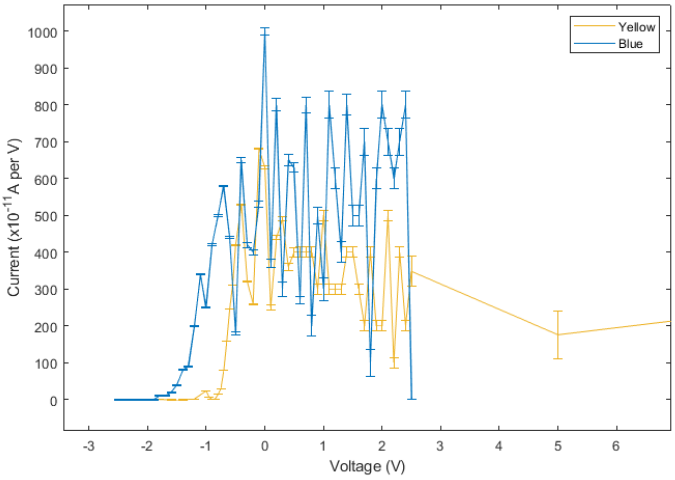

Figure 5: Photoelectron Energy Distribution (Zoomed)

Although the data above is difficult to discern, it is reasonably clear that the photoelectrons from blue wavelengths are consistently more energetic than those created from yellow light as expected by the difference in energy between those wavelengths of light.

5 Discussion

Consistent with the prediction in the theory section, the linear regression of the cut-off voltage against the angular wave number gave a gradient that was used to calculate Planck's constant. Using the appropriate significant figures, this evaluated to

$$\begin{aligned} h &= \frac{2\pi e}{c} m_{Vk} \\ &= \frac{2\pi \times -1.602 \times 10^{-19}\text{C}}{299792458 \text{ m/s}} \times -2.09 \times 10^{-7} \text{ V.m per Cycle} \\ &\simeq 7.02 \pm 0.26 \times 10^{-34} \text{ J.s} \end{aligned} \tag{5}$$

where the uncertainty was propagated according to Appendix C. While this is slightly larger than currently accepted values of $h \simeq 6.626 \times 10^{-34}$ J.s [2], it is within a reasonable range after accounting for the uncertainty in the value.

Looking again at Table 1 (or alternatively Appendix E), the stopping voltage appears to be less negative for lower intensities of light at least by a small margin. As per equation (1) in the laboratory notes, the maximum kinetic energy of a photoelectron is directly proportional to the frequency of incident light from which it was created. Appendix D also shows that the higher range of kinetic energies are far less probable than lower energies. Putting these two ideas together, a lower intensity of light would equate to fewer photoelectrons and, by extension, a lower probability of finding photoelectrons at a higher kinetic energy range. This *could* describe the increase in stopping voltage with reduction in incident light intensity, remaining consistent with the quantum model of light.

Figure 4 shows the expected shape of the current-voltage curve when accounting for the discrepancies between theory and experiment. As per the laboratory notes, the theory for the current-voltage curve for some light frequency would have discontinuities in the derivative of the curve, resulting in sharp changes in the gradient. Predicting the effect of contact potential difference, current leakage and finite temperature resulted in a 'curved' current-voltage curve as seen in the figure. Looking now at Figure 5, photoelectrons created from incident 436nm light consistently had greater kinetic energies than those from 577nm light, suggesting that a higher frequency of incident light corresponds to a higher kinetic energy. This is consistent with equation (1) from the laboratory notes.

The calculated intercept on the linear regression translated to a work function of $\phi = 1.58 \pm 0.94$V for the anode plate. Cross-referencing this against Table 38.1 in Knight (2017), this is far below typical work-function values indicating that the valence electrons within the anode were very weakly bound to their nucleus and didn't require (comparatively) much energy to be broken free into photoelectrons. There are a few possible explanations for this (perhaps the anode was a large molecule, an alloy or significantly negatively charged), but in any case this signifies that the anode was not an ordinarily used metalloid. Worth noting is that, within uncertainty, this work function *could* correspond to elements such as Caesium ($\phi = 1.95$), Sodium ($\phi = 2.36$), Rubidium ($\phi = 2.26$), or some other such metal.

Finally, although some increase in stopping voltage with respect to a reduction in light intensity was observed (as previously alluded to), the increase was not sufficient enough to support a wave-model of light. One would expect that as the light intensity approaches zero, the stopping voltage would also approach zero. This trend was seen, but the gradient of the curve was simply not steep enough to fit with such a prediction. As a result, the photoelectric effect was suggested to follow a quantum model of light in which light energy is transferred through photons, resulting in discrete changes in energy instantaneously.

A possible application of this research lies in space travel. The bulk of the surface area of spacecraft is comprised of elemental metals or alloys which are susceptible to electric charge. Over a prolonged period, I suggest it's probable that incident light from a star could strip the surface of a spacecraft of negative charge leaving metallic ions which could influence onboard electronics. One way to help prevent this would be to either build spacecraft out of, or coat them in a substance with a particularly high work-function, meaning only the most energetic of light would induce the photoelectric effect on the spacecraft. Since the peak of the Sun's emission spectrum lies in the visible, highly energetic wavelengths of light are comparatively sparse (at least in the Solar System) and would increase the longevity of any prospective mission.

6 Conclusions

As a result of two experimental phases investigating the photoelectric effect, multiple constants were determined, as well as a relationship between incident light frequency and the resultant photoelectron kinetic energy distribution. From the first phase of the experiment, using a direct-voltage reading, the stopping voltages for 436nm, 546nm, and 577nm light were used in a linear regression which finally yielded a value for Planck's constant: $h = 7.02 \pm 0.26 \times 10^{-34}$ J.s. By this same regression, a work-function for the bombarded anode was found to be $\phi = 1.58 \pm 0.94$V, which was unlike those referenced in Knight (2017), but consistent within some uncertainty. This discrepancy was attributed to the anode being potentially an anomalous metal.

The second phase of the experiment saw the creation of a current-voltage characteristic curve for the blue and yellow spectral lines of mercury. From this, the photoelectron kinetic energy distributions were plotted and it was found that blue incident light consistently resulted in higher energy photoelectrons, which was attributed to the higher frequency inherent of blue light. Some applications and extrapolations of this investigation were suggested, and ultimately it was found that a quantum model of light was supported from the data collected.

7 Appendices

A Mercury Spectral Lines

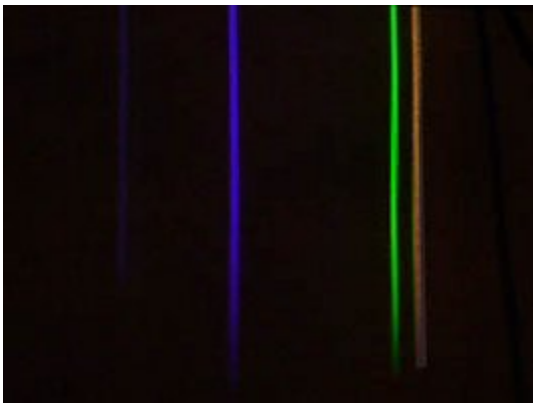

Figure 6: Mercury Spectral Lines

Source: Timichio (Wikipedia) - This file was derived from: HG-Spektrum.jpg, CC BY-SA 3.0, https://commons.wikimedia.org/w/index.php?curid=23246535

B Uncertainty Propagation Table

Relationship	Uncertainty obtained from
General expression	
$p = f(x,y,z,\ldots)$	$(\Delta p)^2 = \left(\frac{\partial f}{\partial x}\Delta x\right)^2 + \left(\frac{\partial f}{\partial y}\Delta y\right)^2 + \left(\frac{\partial f}{\partial z}\Delta z\right)^2 + \ldots$
Specific cases	
$p = x + y$	$\Delta p = \sqrt{(\Delta x)^2 + (\Delta y)^2}$
$p = x - y$	$\Delta p = \sqrt{(\Delta x)^2 + (\Delta y)^2}$
$p = x\,y$	$\frac{\Delta p}{\lvert p\rvert} = \sqrt{\left(\frac{\Delta x}{x}\right)^2 + \left(\frac{\Delta y}{y}\right)^2}$
$p = \frac{x}{y}$	$\frac{\Delta p}{\lvert p\rvert} = \sqrt{\left(\frac{\Delta x}{x}\right)^2 + \left(\frac{\Delta y}{y}\right)^2}$
$p = Bx$	$\Delta p = B\,\Delta x$
$p = Ax^n$	$\frac{\Delta p}{p} = n\frac{\Delta x}{x}$
$p = \log x$	$\Delta p = \frac{1}{2.3x}\Delta x$
$p = \sin\theta$	$\Delta p = \lvert\cos\theta\rvert\,\Delta\theta$

Figure 7: Formulae Used for Uncertainty Propagation

C Example Uncertainty Propagation

In the calculation of Planck's constant (discussion section), the uncertainty propagation was found as follows:

$$\begin{aligned} h &= \frac{2\pi e \cdot m}{c} \\ \Rightarrow \Delta h &= \frac{2\pi e}{c} \cdot \Delta m \\ &= \frac{2\pi e}{c} \cdot 7.6 \times 10^{-9} \\ &\simeq 2.6 \times 10^{-35} \text{ J.s} \end{aligned}$$

And so the calculated value of Planck's constant was

$$h = 7.02 \pm 0.26 \times 10^{-34} \text{ J.s}$$

as per equation 5

D Full Photoelectron Energy Distribution (-2.5 to 30V)

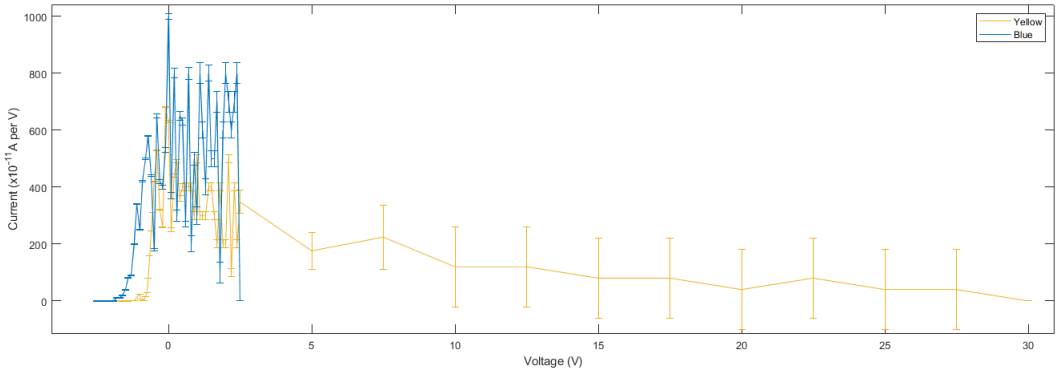

Figure 8: Photoelectron Energy Distribution

E Stopping Voltage-Intensity Curve for Blue Light

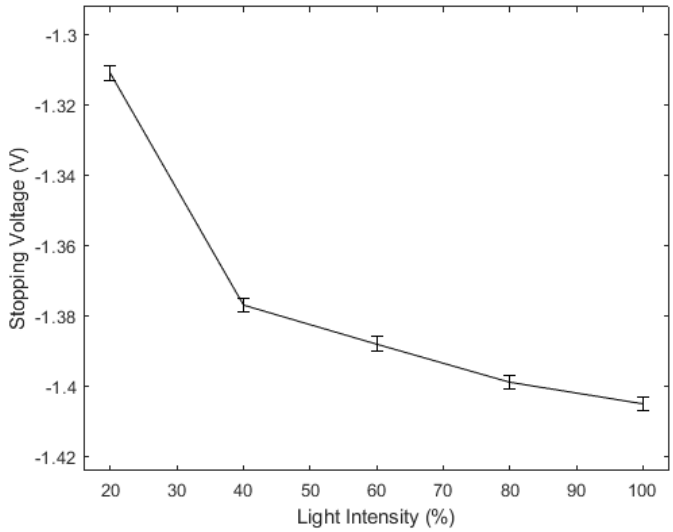

Figure 9: Stopping Voltage vs Incident Light Intensity for 436nm

References

[1] Sauer, T. (2018). *'Numerical differentiation and integration. In Numerical analysis'* (3rd ed., pp. 253-292). Hoboken, New Jersey: Pearson

[2] Knight, R.D. (2017). *'Physics for scientists and engineers: a strategic approach with modern physics (4th ed.)'*. Boston: Pearson.